

# Atomic force microscope (AFM) combined with the ultramicrotome: a novel device for the serial section tomography and AFM/TEM complementary structural analysis of biological and polymer samples

ANTON E. EFIMOV\*, ALEXANDER G. TONEVITSKY†, MARIA DITTRICH‡ & NADEZDA B. MATSKO§

\*NT-MDT Co., Moscow, Russia

†Scientific Research Institute of Transplantology and Artificial Organs, Moscow, Russia

‡Swiss Federal Institute of Aquatic Science and Technology (EAWAG), Kastanienbaum, Switzerland

§Electron Microscopy Centre Zurich (EMEZ), ETH-Zurich, Switzerland

**Keywords.** AFM, cells, microtomy, polymers, TEM, 3D serial section tomography.

## Summary

A new device (NTEGRA Tomo) that is based on the integration of the scanning probe microscope (SPM) (NT-MDT NTEGRA SPM) and the Ultramicrotome (Leica UC6NT) is presented. This integration enables the direct monitoring of a block face surface immediately following each sectioning cycle of ultramicrotome sectioning procedure. Consequently, this device can be applied for a serial section tomography of the wide range of biological and polymer materials. The automation of the sectioning/scanning cycle allows one to acquire up to 10 consecutive sectioned layer images per hour. It also permits to build a 3-D nanotomography image reconstructed from several tens of layer images within one measurement session. The thickness of the layers can be varied from 20 to 2000 nm, and can be controlled directly by its interference colour in water.

Additionally, the NTEGRA Tomo with its nanometer resolution is a valid instrument narrowing and highlighting an area of special interest within volume of the sample. For embedded biological objects the ultimate resolution of SPM mostly depends on the quality of macromolecular preservation of the biomaterial during sample preparation procedure. For most polymer materials it is comparable to transmission electron microscopy (TEM).

The NTEGRA Tomo can routinely collect complementary AFM and TEM images. The block face of biological or polymer sample is investigated by AFM, whereas the last ultrathin section is analyzed with TEM after a staining procedure. Using the combination of both of these ultrastructural methods for the analysis of the same particular organelle or polymer constituent leads to a breakthrough in AFM/TEM image interpretation. Finally, new complementary aspects of the object's ultrastructure can be revealed.

## 1. Introduction

The ability of modern high-resolution electron microscopes to produce images at near atomic resolution has led to tremendous progress in many fields of biological and material research. However, the vast majority of images are 2D projections of a 3D structure. Nowadays the third dimension becomes increasingly important for the comprehensive understanding of the object's ultrastructure (Midgley & Weyland, 2003). In addition, for many applications in biology and polymer science 3D analysis has to be performed within a layer of up to several hundred micrometers thick.

At present 3D structure can be reconstructed with the resolution in the nanometers range using either tilt-series-based or serial ultrathin sections tomography. A tilt-series-based tomography can be obtained with transmission electron microscopy (TEM) (Horowitz *et al.*, 1997; Medalia *et al.*, 1997; Perkins *et al.*, 1997), transmission X-ray microscopy (TXM) (Kaestner *et al.*, 2003; Sutton *et al.*, 2003), energy-filtered TEM (EFTEM) (Midgley & Weyland, 2003), atom probe field ion

Correspondence to: Dr. Nadezda B. Matsko, Forschungsinstitut für Elektronenmikroskopie, und Feinstrukturforschung (FELMI-ZFE), Steyrergasse 17, A-8010 Graz, Austria. Tel: +43 (0)316 8738335; fax: +43 (0)316 811596; e-mail: nadezda.matsko@felmi-zfe.at

microscopy (APFIM) (Miller, 2000) and high-angle annular-dark field scanning transmission electron microscopy (HAADF STEM) (Koguchi *et al.*, 2001).

Serial ultrathin sections tomography is based on 3D TEM (Howard & Ems, 1984) or AFM (Chen *et al.*, 2005) reconstruction of serial ultrathin sections or, alternatively, block-face imaging combined with serial sectioning inside the chamber of a scanning electron microscope (SEM) (Denk & Horstmann, 2004; Heymann *et al.*, 2006). The sectioning procedure can be also performed using focused ion beams (FIB tomography) (Holzer *et al.*, 2004).

However, these currently available methods have drawbacks that limit their applications. Thin samples in the 100-nm range are necessary for a tilt-series-based tomography. This requirement complicates the application of these methods for reconstruction of larger volume structures. Furthermore, the necessity to use only electron- and photon-transparent materials strictly limits the number (types) of specimens, which are acceptable for such analysis.

Serial ultrathin sections tomography is suitable for the reconstruction of the large specimens. However, this method faces two severe problems. First, serial sections preparation here is very time-consuming. Second is a low electron microscopy contrast of biological and polymer materials because the light elements they consist of scatter the incident electrons rather weakly. The first problem may be solved by complete automation of the microtomy (Denk & Horstmann, 2004). Applying high voltages, and staining may enhance the weak scattering. However, high voltages usually lead to the beam damage of the samples. Staining of the whole sample can considerably improve the contrast, but the heavy metal salts, which are used for such purpose have a finite size and can penetrate deep into the sample only when the cellular macromolecule matrix are partially or completely removed. Therefore only those fixation methods, which are aggressive to macromolecules like classical chemical fixation followed by rapid dehydration, can provide a sufficient block staining of biological samples (Hunziker *et al.*, 1984; Hayat, 2000). For polymer samples staining with different chemicals (e.g. OsO<sub>4</sub>, RuO<sub>4</sub>) is normally used. However, this procedure can change the native structure of the phases (Sawyer & Grubb, 1996). Therefore, the block staining for EM is one of the most serious limitations for the gentle fixation of the biological tissue/polymer composites, and, thus, for their proper structural preservation.

By contrast, the analysis of the block face of polymer materials with AFM does not require the staining of the specimen. The reason for this is the different principle of an image contrast formation in EM and AFM. In EM an image contrast is formed by the sufficiently scattering structures from 15- to 90-nm-thick volume of a section (TEM analysis) or 10–100 nm surface layer of block (SEM analysis at low energies) (Reimer, 1993). As a result, only the cell constituents, which react with the staining agents, and which

can be reached by the latter, are detected. Where as, image contrast in the AFM is due to a height corrugation or a phase shift generated by surface inhomogeneities (Matsko & Mueller, 2004). Such inhomogeneities appear on the surface of the block face due to copolymerized cell components (mainly macromolecules) (Matsko, 2006). All of them can be observed without staining on the plane of the section, and not in the 2D projection, like with TEM. Consequently, the correlative AFM/TEM structural analysis provides new ultrastructural aspects of a macromolecular arrangement of a biosamples.

In this article we describe a new instrument (NTEGRA Tomo), which is based on the integration of NT-MDT's NTEGRA SPM platform and the Leica UC6NT ultramicrotome. Our goal was to develop the device, which enables the direct monitoring of the block face structure of the specimen while it is within the cycle of the ultramicrotome sectioning procedure. This combination of instruments has an advantage in the fast search of an area of special interest of the sample by scanning the block face each time a layer was removed by the microtome knife. The efficiency of this area detection for biological specimens depends on the quality of their macromolecular preservation during sample preparation procedure. For most polymer materials it is comparable with TEM.

Three-dimensional reconstruction in the NTEGRA Tomo can be obtained by automated block-face imaging combined with serial sectioning by the ultramicrotome. The step size can be varied from 20 to 2000 nm according to the microtome adjustments, and can be controlled directly by its interference colour in the water. Automation and optimization of sectioning/scanning cycle allow one to acquire up to 10 consequent layer images per hour and to perform the nanotomography from several tens of layer images within one measuring session.

With this new instrument (the NTEGRA Tomo) TEM and AFM complementary pairs of images can be routinely prepared and analyzed. The block face of the biological or polymer sample was prepared for AFM while the last ultrathin section was collected, post-stained and used for TEM. Finally the same ultrastructure will be investigated by two complementary methods, allowing for correspondence of stained structure and their macromolecular/phase composition.

## 2. Materials and methods

### 2.1. High-pressure freezing

Adult *C. elegans*, kind gifts of Prof. M. Gotti, ETH Zürich, and cyanobacteria *Synechococcus* PCC 7942, from chemostate cultures grown in Z/10 medium were washed (Dittrich and Sessler, 2005; Obst *et al.*, 2006) and high-pressure frozen as described earlier (Hohenberg *et al.*, 1994).

Life cat's mite *Otodectes cynotis* was mounted in aluminium platelets filled with hexadecane and immediately frozen.

All freezing procedures were performed by a HPM 010 high-pressure freezer (Bal-Tec, Principality of Liechtenstein).

## 2.2. Freeze-substitution and embedding

Epoxy freeze-substitution was performed in water-free acetone containing 15% of the complete Araldite/Epon formulation [49% w/w Araldite/Epon stock solution, 49% w/w Hardener DDSA (Fluka) and 2% w/w Accelerator DMP-30 (Fluka)]. The Araldite/Epon stock solution consisted of 41% w/w Epoxy-Einbettungsmittel (Fluka), 54% w/w Durcupan ACM (Fluka) and 5% w/w Dibutylphthalate (Fluka)].

The standard freeze-substitution regime, where the samples were kept at  $-90^{\circ}\text{C}$ ,  $-60^{\circ}\text{C}$  and  $-30^{\circ}\text{C}$  for 8 h at each temperature, and finally warmed to  $0^{\circ}\text{C}$ , was used (Van Harreveld & Crowell, 1964). Between the steps, the temperature was raised by  $1^{\circ}\text{C}/\text{min}$ .

All samples were embedded in Araldite/Epon embedding mixture. Infiltration was performed stepwise (33% resin in water-free acetone for 4 h, 66% resin in acetone for 4 h, 100% resin overnight in a desiccator evacuated with a membrane pump to 10 mbar to maintain dry conditions). All samples were polymerized at  $60^{\circ}\text{C}$  for 3 days.

## 2.3. Transmission electron microscopy

Ultrathin sections (10–50 nm) were obtained using a Leica Ultracut Emicrotome (Leica, Austria) equipped with a diamond knife (Diatome, Switzerland). Sections for TEM analysis were collected on kolloidum/carbon coated grids, stained with uranyl acetate and lead citrate (Reynolds, 1963) and examined in a EM 912 Omega (Zeiss, Oberkochen BRD) electron microscope equipped with a ProScan  $1\text{ k} \times 1\text{ k}$  slow scan CCD camera (Proscan, Munich, BRD).

## 3. Results and discussion

### 3.1. AFM head – principle and construction

To achieve the goals outlined in the Introduction, a special AFM head was designed. This AFM head is placed directly on the ultramicrotome (Leica UC6NT series) knife holder over the knife. This construction allows the investigation of the block face surface when the ultramicrotome arm is in the highest position. The principle of combined AFM and UMT operation is shown on Fig. 1.

The cantilever tip scans the block face surface using a horizontally oriented piezotube scanner with the scanning range of  $100 \times 100 \times 10\text{ }\mu\text{m}$ . The scanner is equipped with capacitance displacement sensors for all three coordinates and has the closed-loop control of probe positioning in the scanning plane. To detect the probe displacement we use standard optical cantilever deflection registration system, which consists of a semiconductor laser and a four-section photodiode.

The major components of the instrument are illustrated in Fig. 2. AFM head with three support legs is clamped with spring

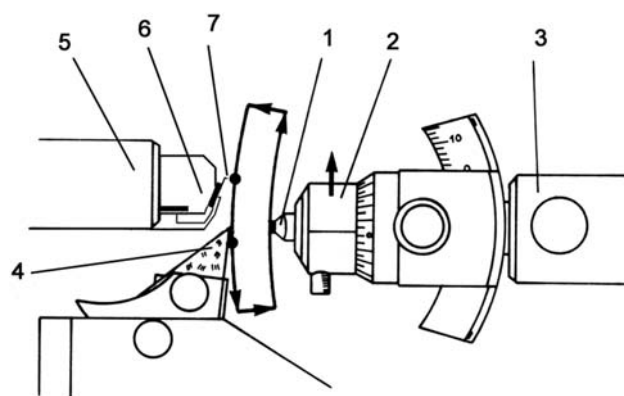


Fig. 1. Schematic illustration of a combination of AFM measuring system, with sectioning part of the microtome. 1 – sample; 2 – sample holder; 3 – ultramicrotome arm; 4 – ultramicrotome knife; 5 – AFM scanner; 6 – holder for AFM probe and 7 – AFM probe.

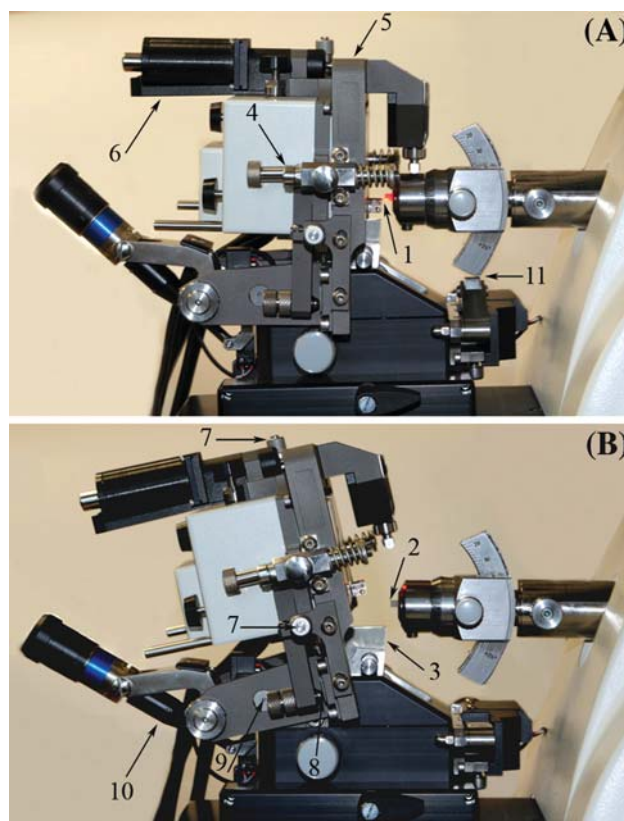
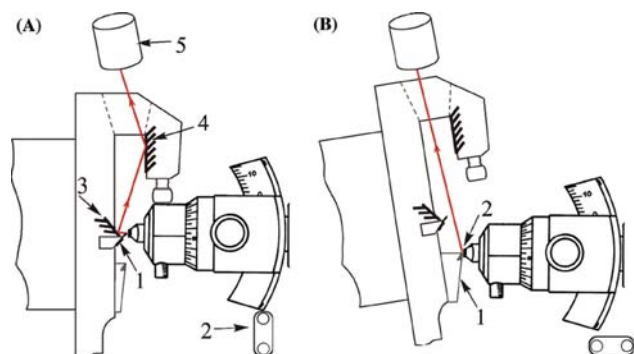


Fig. 2. NTEGRA Tomo AFM head in measuring (A) and sectioning (B) positions. 1 – AFM probe; 2 – sample; 3 – ultramicrotome knife; 4 – spring locks; 5 – support platform; 6 – stepper motor for probe approach; 7 – positioning microscrews; 8 – polysapphire plate; 9 – support pivots; 10 – motorized rear screw and 11 – ultramicrotome arm support.



**Fig. 3.** Optical system of the NTEGRA Tomo in measuring (A) and sectioning (B) position. (A) 1 – probe holder; 2 – ultramicrotome arm support; 3 – mirror on the AFM head; 4 – mirror on the support frame and 5 – stereomicroscope objective lens; (B) 1 – ultramicrotome knife and 2 – sectioned sample.

locks to the massive titanium frame. The upper leg of the AFM head is equipped with the stepper motor to control the coarse approach of the probe to the block face surface. The position of the probe on the plane of the sample surface is defined by two perpendicular microscrews allowing manual positioning of the probe relative to the sample in a range of 4–8 mm. We use support legs with spherical endings that are pressed against polished polysapphire plates to minimize friction in the XY coarse positioning of the head.

The frame is hinged at the two opposite symmetrical support pivots based on the knife holder and can be turned around corresponding axis by the stepper motor. This hinging out ensures optical access for the ultramicrotome optics to the knife-edge area during sectioning. Basically the system has two positions. A microtome operating position and an AFM measuring position. (Fig. 2A) is when the AFM probe is scanned on the block face and sectioning position. (Fig. 2B) is when the AFM head is lifted up on the pivots and ultramicrotome operates in its regular regime.

The system of mirrors (Fig. 3) on the AFM head and support platform of the frame enables to use original (Leica MZ6) binocular optical microscope of Leica UC6NT ultramicrotome both for positioning of the AFM probe on the block face during measurements (Fig. 3A) and for direct observation of the sample and knife edge in sectioning position (Fig. 3B).

One of the main problems to solve in this design was the minimization of mechanical noises in the tip-sample system. This is crucial for the accurate / stable AFM measurements. If the microtome arm and the AFM head are not coupled mechanically, the RMS noise in Z direction in such system may achieve the value of 1 nm, which is far beyond the satisfactory level for the AFM.

In order to establish the mechanical coupling of UMT arm and AFM head we have introduced the support prong of the AFM holding frame, which leans on the ultramicrotome sample holder when the system moves into the measuring

position. The sample holder itself stands on the removable support, which could be moved up and down to the fixed positions by a motorized system. This construction provides a minimum of mechanical noise in the tip-sample system to the level of 0.05 nm RMS. This was due to the increased stiffness of the mechanical system improving the resonant frequencies. However, our experiments show that the inclusion of an active vibration isolation system (like Hertzian TS-1 50) is still necessary for the decent results.

The removable support for the ultramicrotome sample holder also plays a role in the fixation for the sample holder in the vertical direction. As we intend to return and perform AFM measurements in the same area of the block face after each section the mechanically defined fixation of the sample position is significant.

### 3.2. Controlling electronics and software

The system utilizes the standard NTEGRA SPM controller and Nova RC1 version 1.0.26.997 (or higher) acquisition and image processing software by NT-MDT. The standard configuration allows for making measurements in all of conventional AFM modes including: contact AFM, LFM, semi-contact AFM, phase imaging, contact and semi-contact feedback-error modes, MFM and a number of electrical measuring techniques (EFM, SKPM, Spreading Resistance Imaging). However, our experiments demonstrate that the most informative measuring technique for revealing the ultrastructure of polymer and epoxy embedded biological samples is the phase imaging mode. This mode is a logical choice because we could not expect useful topography information from the block face, which is supposed to be sectioned as flat as possible. However, the AFM phase imaging contrast is generated by local variation of viscoelastic properties of the sample and this mode is non-destructive for the polymer samples (Magonov & Reneker: 1997).

The operation of ultramicrotome arm and AFM head movements as well as AFM measurements can be controlled from the Nova software and automated with use of Nova Powerscript™ macro language scripts. UC6NT ultramicrotome arm movements are controlled by the software via special RS232 interface developed by Leica Microsystems GmbH for this purpose. This automation sufficiently eases the acquisition of numerous consecutive frames necessary for 3D reconstruction.

Another difficulty for the 3D-reconstruction of nanostructures is the alignment of consecutive AFM images in the X-Y (scanning) plane. The problem is that the ultramicrotome arm and the AFM probe do not return exactly in the same place after each section and such misalignment may be of the order of microns. We use ImagePro Plus 5.1 post-processing software by Media Cybernetics, Inc., with 3D Constructor option for the automatic image alignment and visualization of 3D voxel images.

### 3.3. Identification of specified area of interest within the sample

The investigation of the ultrastructural aspects of the biological objects often requires finding an area of interest for TEM analysis within a large volume or area of the sample. Sometimes the searching procedure becomes extremely complicated, especially when the goal is to detect the tiniest cellular details like local networks of neurons or rarely distributed phases/defects within polymer composites. The thing that contributes to this effect is a disability to make a primary screening of the area of a sample, which is currently under the sectioning, with the resolution comparable to TEM. Till now the rough screening is performed through light microscope (LM) (semi-thin sections) (Roessler *et al.*, 1991; Schwarz, 1994) or confocal laser scanning microscope (CLSM) (block face) (Biel *et al.*, 2003). For the latter a fluorescent dye should be included in early steps of a sample preparation procedure. Such techniques allow one to detect structural details not smaller than a several hundreds of nanometers, and cannot be used for the observation of most of cellular constituents, bacteria etc. For polymers such methods cannot be used at all due to absence of the intense fluorescent labelling within a sample volume.

Therefore, a more sophisticated approach to find the area of interest is based on usual ultrathin section preparation following to TEM examination. However, such procedure sometimes takes weeks of a hard work and never gives the guarantee of success.

The automatic AFM imaging of the block face of the sample each time before the next sectioning helps to identify the precise area of interest relatively quickly. The instrument characteristics (probe geometry and planar interface, signal-to-noise ratio) allow one to access structural details on a sub-nanometer scale (Mou *et al.*, 1995; Walters *et al.*, 1996; Walz *et al.*, 1996; Reviakine *et al.*, 1998; Scheuring *et al.*, 1999; Schmitt *et al.*, 2000). Nevertheless, an ultimate resolution of biomolecule or organelle architecture is determined by its topographical and/or phase profile in a context of the whole cell structure (Matsko, 2006). Therefore the preservation of biomacromolecule integrity during sample preparation procedure becomes extremely important for the high resolution AFM. Figures 4(A), (C) and 5(A) show the AFM phase image and Figs. 4(B), (D) and 5(B) corresponding TEM micrographs of the freeze-pressure frozen and epoxy freeze-substituted *C. elegans* (Fig. 4) and cyanobacteria *Synechococcus* (Fig. 5). It is known that such sample preparation procedure provides almost the best macromolecular preservation of the biosamples, and can be used successfully both for AFM and TEM investigation of cellular ultrastructure (Matsko, 2005). AFM images show that the identification of the most of the cellular organelles (nuclei, mitochondria, ribosomes, hypodermal structures) can be implemented with a good precision.

For polymer samples the AFM resolution mainly depends on viscoelastic properties of the surface under investigation. The facilities of the NTEGRA Tomo AFM can work at the different scanning regimes (phase imaging, contact and semi contact feedback-error modes, MFM and a number of electrical measuring techniques), simplifying effectively depict surface properties of the investigated materials. Therefore, it makes searching of the place of interest ease.

### 3.4. AFM-TEM complementary pairs of images

Although the high-resolution electron microscopy of the ultrathin sections of embedded biological materials provides information about morphology and location of the stained cellular constituents within the cell, the atomic force microscopy is a valid approach for assessing their macromolecular content and architecture (Matsko, 2006). Therefore, the full picture emerges only when results from different methods are combined.

The discussed AFM/ultramicrotome system allows one to make correlative AFM/TEM analysis of particularly the same place on the specimen routinely by two microscopic methods. Here, the crucial point is that one particular organelle or biomolecule can be cut into two parts, one part being used for AFM and another one for TEM. For AFM, we used the block-face of epoxy fixed and embedded mite (Fig. 6A), while the last ultrathin section was collected, post-stained with uranyl acetate and lead citrate, and then used for TEM (Fig. 6B). Such complementary pair of images both enables the adequate interpretation of the AFM images (which may be complicated due to a lack of accumulated knowledge about the AFM appearance of most of the cellular constituents), and the revealing a new ultrastructural aspects of macromolecular arrangement in a cell, going beyond the possibilities offered by AFM or TEM alone.

Under conventional conditions, when AFM and microtome are separated, the procedure of complementary pair of images preparation is extremely complicated. The resin embedded specimen first should be re-embedded in a special microholder, which at the same time fits the microtome and is suitable for the examination of the block face by AFM. After sectioning, one should remove the sample block from the microtome, and mount it in the working space of the atomic force microscope. The whole procedure should be done without mechanical disturbance of the sample surface. This is not so easy because everything must be done manually on the micro level. Next is to collect and stain the last ultrathin section to make it accessible for TEM analysis. This procedure requires very accurate and precise work, as one mistake will make the whole experiment unsuccessful. Therefore, at most, what can be expected during microtome session is one complementary set of images.

With the NTEGRA Tomo there are no problems with the block face handling, because the new device does not require



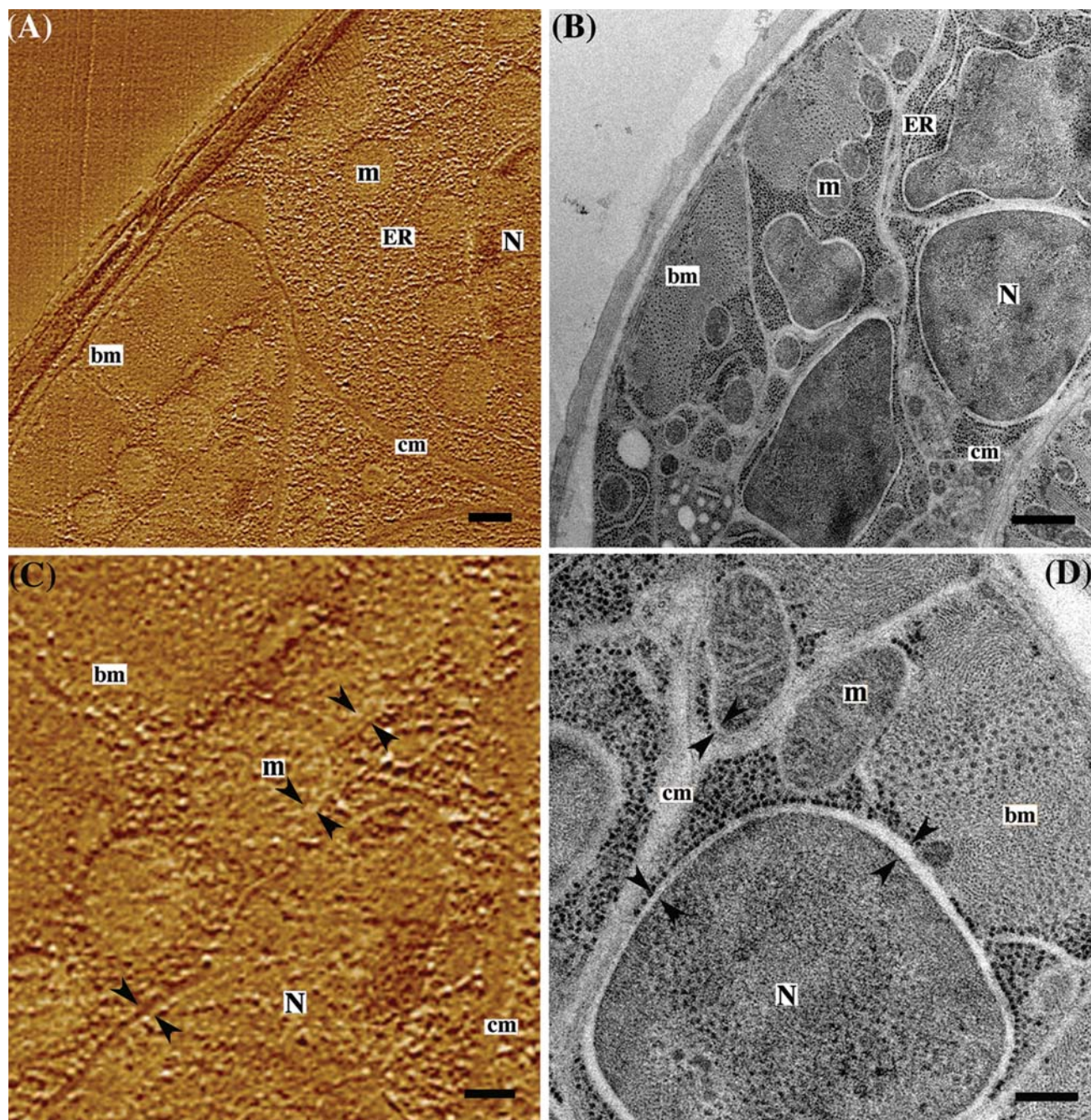


**Fig. 4.** Corresponding (A, C) AFM phase (block face) and (B, D) TEM (ultrathin section) images of the cross section of the adult *C. elegans* which are high-pressure frozen and freeze-substituted in acetone containing 20% Epon/Araldite mixture. Black arrows point to mitochondrial and nucleus membranes. Phase variation:  $0^{\circ}$ – $15^{\circ}$  in (A, C). Scale bars equal 500 nm in (A, B), and 200 nm in (C, D). N nucleus, m mitochondria, bm body-wall muscles, ER endoplasmic reticulum, cm cell membrane.

a special holder for AFM examination, and after sectioning the procedure of AFM approaching the block face surface is done automatically. The ultrathin section preparation remains almost the same. However, the efficiency of the complementary set of image preparation is greatly increased due to the

increased ability to produce several AFM images of the block face during one microtome session (consequent AFM scanning – section preparation). At the end of microtome session one can have several ultrathin sections, which have been already analyzed by the AFM, and a few of them can be well situated on



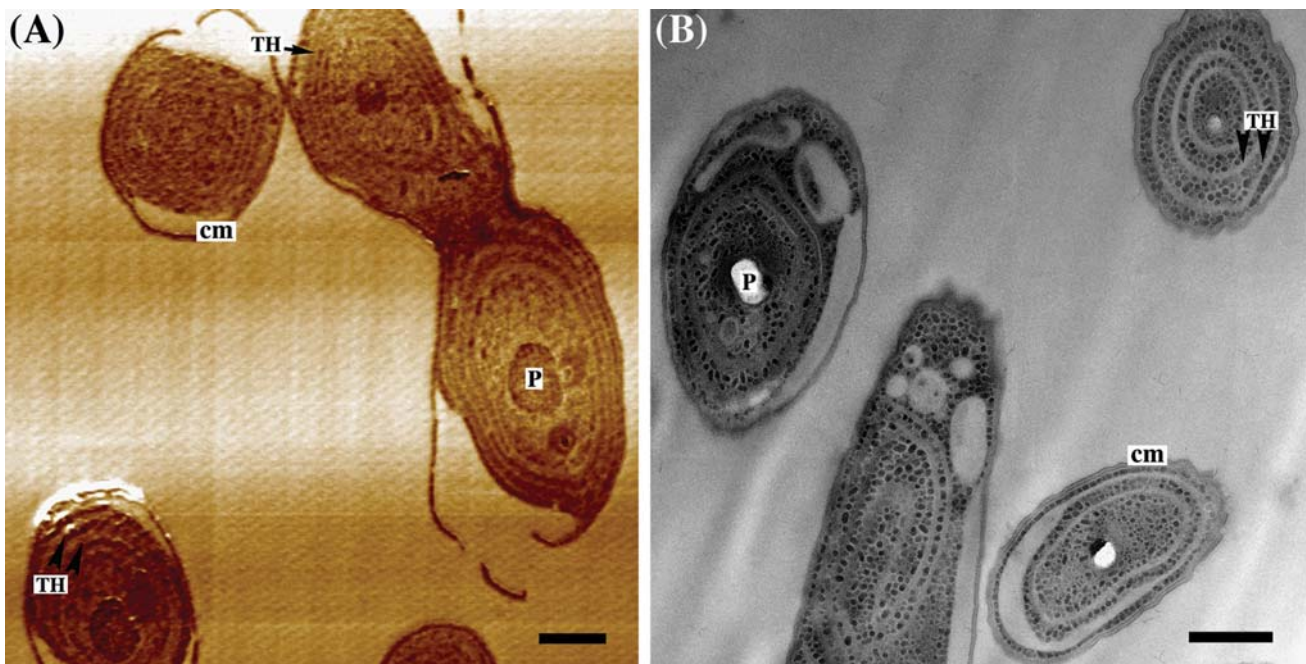


Fig. 5. Corresponding (A) AFM phase (block face) and (B) TEM (ultrathin section) images of cyanobacteria *Synechococcus* which are high-pressure frozen and freeze-substituted in acetone containing 20% Epon/Araldite mixture. Phase variation:  $0^{\circ}$ – $20^{\circ}$  in (A). Scale bars equal 500 nm. TH thylakoid, P polyphosphate granule.

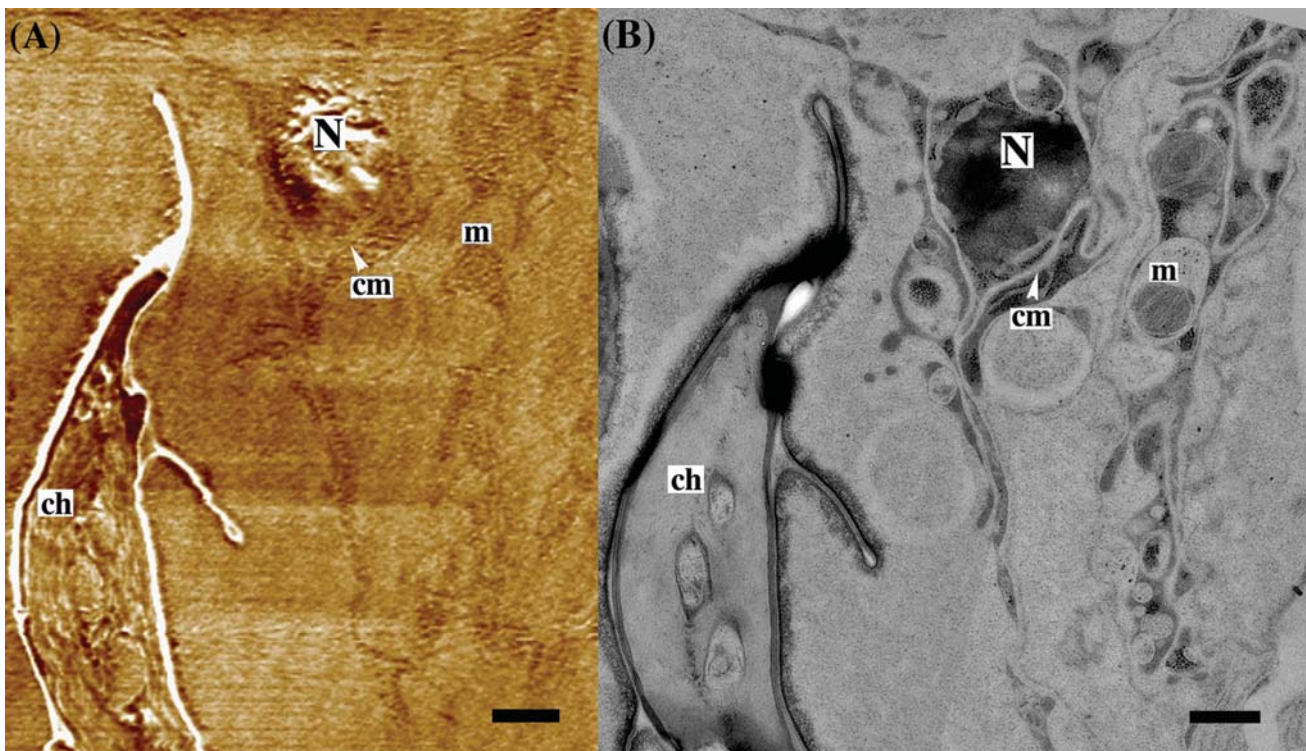


Fig. 6. AFM phase (A)/TEM (B) complementary pairs of images of a longitudinal section of cat's mite *Otodectes cynotis*, high-pressure frozen and freeze-substituted in acetone containing 20% Epon/Araldite mixture. Phase variation:  $0^{\circ}$ – $4^{\circ}$  in (A). Scale bars equal 500 nm. N nucleus, m mitochondria, cm cell membrane, ch chitin.

the grid and properly stained to allow them to be successfully examined by TEM.

### 3.5. 3D image reconstruction and control of section thickness

AFM 3D structural analysis (analogous to the serial sectioning TEM reconstruction) implies that the sections are imaged before being cut, i.e. by repeatedly scanning the block face. Two important technical requirements for this technique should be mentioned.

First is the alignment of the images with regard to their displacement in the scanning plane. The  $x$ - $y$  displacement of the probe-sample relative position is generated by a number of factors including: mechanical repeatability of the system positioning, thermal and other drifts and block face relaxation after sectioning. The total mismatch of the images from frame to frame may reach several microns. We utilize ImagePro Plus 5.1 3D Constructor software for automatic image alignment by a correlation-based algorithm. For 3D reconstruction on a smaller scale when the scan size is comparable to typical mismatch values we were first acquiring the larger area overview image in order to locate the feature of interest and then zooming in on the smaller area. As the AFM scanner of NTEGRA Tomo is equipped with closed loop control based on capacitance sensors the measurement does not introduce any significant additional error.

The second important requirement is the control of section thickness. This is still a limiting factor for high-resolution 3D imaging via ultramicrotomy. After sectioning AFM measurements still take 5–10 min and, therefore, thermal drift and block face relaxation can lead to errors comparable with the thickness of ultrathin (10–50 nm) section. However there is a well-established technique for section thickness control based on optical detection of the interference colour in light reflected from the section while it is floating on the surface of a liquid in the knife trough (Hayat, 2000). Moreover this technique is the only one, which enables one to directly measure the thickness of the section during sectioning procedure with accuracy of a 10-nm range. The AFM head construction allows one the optical access to the knife-edge area during sectioning, thus colours of the sections may be observed in the regular way. To systematize section colour data video images from the optical microscope after each section can be acquired and stored in the computer. The Nova image database system (NT-MDT) allows one to assign an optical image to a corresponding AFM image. Then even if section thickness varies from one 2D image to another this information is still available for the software analysis and reconstruction.

Figure 7 illustrates the AFM 3D reconstruction of ABS/PA6 (Acrylonitrile-butadiene-styrene/polyamide 6) polymer blend structure. No special sample preparation was performed on ABS/PA6 samples besides regular ultramicrotome trimming. Serial acquisition of consequent phase images was performed in automatic regime controlled by macrolanguage software

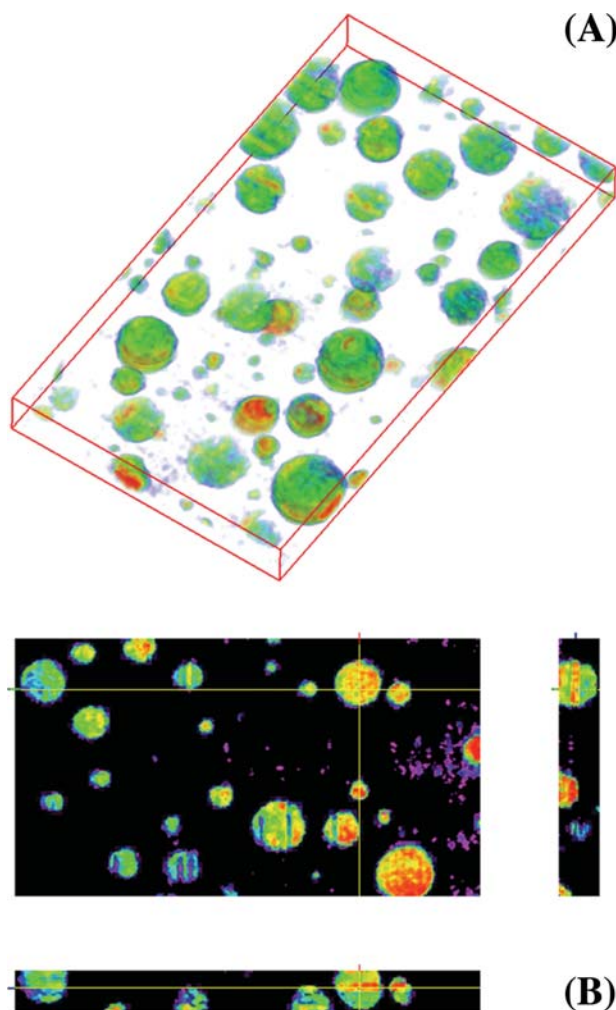


Fig. 7. 3D AFM reconstructed ABS/PA6 (Acrylonitrile-butadiene-styrene/polyamide 6) polymer blend structure. The green phase reveals submicron spherical clusters of ABS in PA6 matrix. The resulted volume image contains  $350 \times 200 \times 25$  voxels what corresponds to physical size of  $8.75 \times 5.0 \times 1.0 \mu\text{m}$ . (B) Orthogonal slices of the ABS/PA6 for 3D visualization. The ImagePro Plus 5.1 3D Constructor software was used for the automatic image alignment by the correlation-based algorithm.

script without any additional adjustments. Thus final area cut off of  $7.5 \mu\text{m}$  in vertical and  $3.75 \mu\text{m}$  in horizontal directions correspondingly gives an idea of resulting frame-to-frame probe positioning accuracy that is defined by the mechanical stability of the system and by the drifts of various origin. Average acquisition time per one sectioning-measuring cycle was about 6 min. We have acquired 25 consequent  $512 \times 512$  pixels AFM phase images of the  $12.5 \times 12.5 \mu\text{m}$  block face area after ultramicrotome sectioning with set section thickness of 40 nm. An obtained series of 25 frames was processed with use of ImagePro Plus 5.1 3D Constructor software for automatic image alignment and visualization of



3D voxel image. The resulting volume image contains  $350 \times 200 \times 25$  voxels, which corresponds to a physical size of  $8.75 \times 5.0 \times 1.0 \mu\text{m}$ . The 3D volume image reveals sub-micron spherical clusters of ABS in PA6 matrix. Assuming that the polymer blend structure is isotropic and ABS clusters are spherical we can also have here an inherent proof of correctness 3D reconstruction. The regular circle shape of ABS clusters observed in the  $z$ - $x$  and  $z$ - $y$  plane sections of reconstructed 3D volume image proves that the 40 nm uniform spacing between the layers we used is a reasonable approximation.

The AFM 3D tomography can be equally useful for biological objects, embedded in epoxy resin. The absolute requirement for this is the prime preservation of the macromolecular content of the biological object, which guarantees the proper AFM image quality. Figure 8 represents the example of AFM 3D reconstruction of a high pressure frozen and epoxy freeze-substituted cyanobacteria *Synechococcus*. The resulting volume image contains  $432 \times 398 \times 6$  voxels what corresponds to physical size of  $2.7 \times 2.5 \times 0.15 \mu\text{m}$ . Figure 9 shows dislocation of the plasma membranes within the bacterial volume. It should be noted that the interpretation of AFM images of biological objects is not trivial. In TEM of ultrathin sections the cell organelles can be identify from their well-defined TEM profile. The profile forms due to different stainability of macromolecules and other molecules, which are involved in the organelle structure (like RNA in a ribosomes,



**Fig. 8.** Surface visualization of the AFM 3D reconstructed cyanobacteria *Synechococcus*, which was high-pressure frozen and epoxy freeze-substituted. The resulted volume image contains  $432 \times 398 \times 6$  voxels what corresponds to physical size of  $2.7 \times 2.5 \times 0.15 \mu\text{m}$ . The ImagePro Plus 5.1 3D Constructor software was used for the automatic image alignment by the correlation-based algorithm.

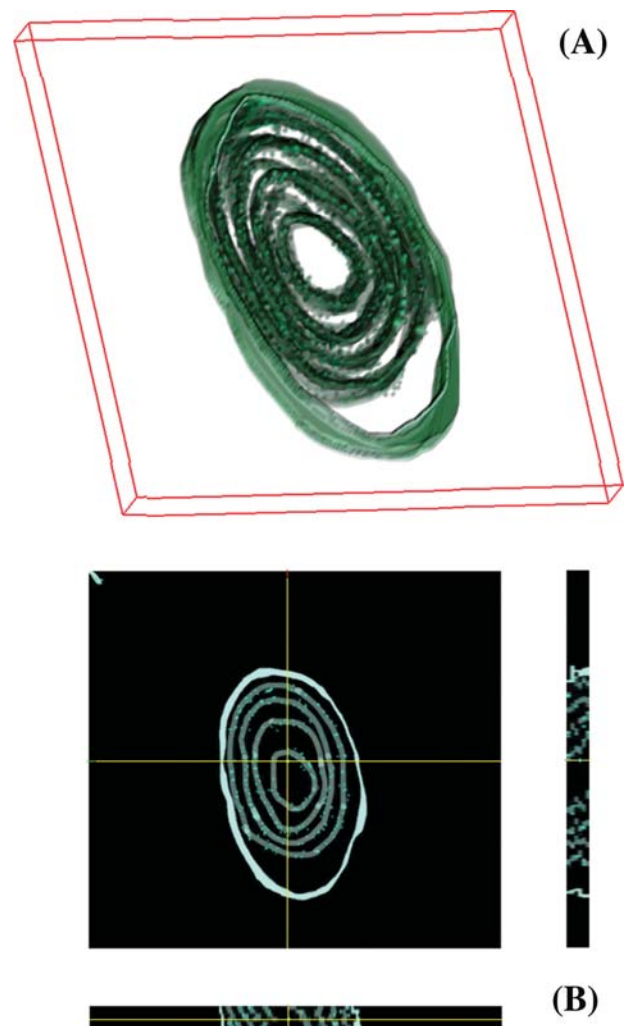


**Fig. 9.** Dislocation of the plasma membranes within the same subvolume of cyanobacteria as in Figure 8. (B) Orthogonal slices of the *Synechococcus* for 3D visualization. The ImagePro Plus 5.1 3D Constructor software was used for the automatic image alignment by the correlation-based algorithm.

lipids in membranes, actin/myosin in a muscles, etc). The stained molecules in 2D projection of near 30–90 nm thick layer of section produces TEM contrast. AFM in contrast to TEM, allows for a direct detection of the copolymerized cells components (mainly macromolecules) directly on the plane of the section, and do not use staining agent at all. Therefore, in TEM image of the cyanobacteria one can detect intensively stained lipid bilayer of plasma membrane (Fig. 5B), when in AFM image the membrane could be identified from the more dense macromolecule content (compare with the rest of cytoplasm) (Figs. 5A and 8). But if an organelle does not have specific macromolecule structure (in terms of their ease to identify shape and consistency), it could be very difficult to find it on the AFM image. The difficulties with the interpretation of the AFM image surely have influence on

the interpretation of the whole AFM 3D tomography profile. From our point of view, this is the only limitation to using 3D AFM tomography routinely in biology. Nevertheless, the unique opportunity provided by AFM in the detection of the macromolecular distribution within cell volume leads to a deeper understanding of entire cellular ultrastructure, going far beyond the possibility offered by TEM alone. This one-to-one correspondence of stained structure and their macromolecular composition in three dimensions should give the biologist a very powerful method to analyze nanoscale biostructure in the future.

#### 4. Conclusion

Using a combination of different imaging methods in structural biology or polymer science almost always gives more, than each method alone. The new instrument described here, the NTEGRA Tomo, which is the conjugation of the conventional SPM with the microtome, is the good illustration of such an idea. Apart from facilities, offered by each of these instruments, the NTEGRA Tomo provides a number of additional options, which can be appreciated in ultrastructural investigation on a wide range of biological or polymer materials.

The first is the use this instrument for Serial Section Tomography. 3D reconstruction in the NTEGRA Tomo can be obtained by automated block-face imaging combined with serial sectioning by the ultramicrotome. The step size can be varied from 20 to 2000 nm thick, the sectioning/scanning cycle permitted to acquire up to 10 sequential images per hour and to obtain the nanotomography image reconstructed from several tens of layer images within one measuring session.

The second is that the NTEGRA Tomo is a valid instrument for the precise detection (imaging) of an area of special interest within the volume of the sample with resolution on a nanometers scale. Although for embedded biological objects an ultimate resolution of SPM depends mostly on the quality of macromolecular preservation of the biomaterial during sample preparation procedure, for most of polymer materials it is comparable to TEM.

The possibility to routinely produce AFM/TEM complementary sets of images for the correlative ultrastructural analysis of the biological or polymer materials is the third evident advantage of the NTEGRA Tomo. The NTEGRA Tomo is proving to be an exciting tool, which is equally useful for the routine measurements of processes such as sample quality control, and for the more complex scientific sample investigations.

#### Acknowledgements

We are very grateful to NT-MDT workshop for precision machining, Leica Microsystems, Austria, and NT-MDT computer group for the development of electronic hardware and fruitful collaboration, Viktor Bykov, Sergey Saunin, Dmitriy Sokolov for fruitful discussions. We would like to thank

Martin Mueller for his decisive support during this work. The help provided by Andrey B. Matsko, Marshall W. Bates and Artem Rudenko in the preparation of the manuscript is also highly appreciated.

#### References

- Biel, S.S., Kawaschinski, K., Wittern, K.P., Hintze, U. & Wepf, R. (2003) From tissue to cellular ultrastructure: closing the gap between micro- and nanostructural imaging. *J. Microsc.* **212**, 91–99.
- Chen, Y., Cai, J., Zhao, T., Wang, C., Dong, S., Luo, S. & Chen, Z.W. (2005) Atomic force microscopy imaging and 3-D reconstructions of serial thin sections of a single cell and its interior structures. *Ultramicroscopy*, **103**, 173–182.
- Dittrich, M. & Sibling, S. (2005) Characterizing of cell surface groups of two picocyanobacteria strains. *J. Coll. Interface Sci.* **286**, 487–495.
- Denk, W. & Horstmann, H. (2004) Serial block-face scanning electron microscopy to reconstruct three-dimensional tissue nanostructure. *PLoS Biol.* **2**(11), 1900–1909.
- Hayat, M.A. (2000) *Principles and Techniques of Electron Microscopy: Biological Applications*, 4th ed. Cambridge University Press, New Jersey.
- Heymann, J., Hayles, M., Gestmann, I., Giannuzzi, L., Lich, B. & Subramaniam, S. (2006) Site-specific 3D imaging of cells and tissues with a dual beam microscope. *J. Struct. Biol.* **155**(1), 63–73.
- Hohenberg, H., Mannweiler, K. & Mueller, M. (1994) High-pressure freezing of cell suspensions in cellulose capillary tubes. *J. Microsc.* **175**(1), 34–43.
- Holzer, L., Indutnyi, F., Gasser, P., Münch, B. & Wegmann, M. (2004) Three-dimensional analysis of porous BaTiO<sub>3</sub> ceramics using FIB nanotomography. *J. Microsc.* **216**, 84–95.
- Kaestner, A., Lehmann, P., Wyss, P. & Flühler, H. (2003) Synchrotron tomography to map the pore structure of sandsamples. *Geophys. Res. Abstracts*, **5**, 11095.
- Koguchi, M., Kakibayashi, H., Tsuneta, R., Yamaoka, M., Niino, T., Tanaka, N., Kase, K. & Iwaki, M. (2001) Three-dimensional STEM for observing nanostructures. *J. Electron Microsc.* **50**, 235–241.
- Matsko, N. & Mueller, M. (2004) AFM of biological material embedded in epoxy resin. *J. Struct. Biol.* **146**, 334–343.
- Matsko, N. & Mueller, M. (2005) Epoxy resin as fixative during freeze-substitution. *J. Struct. Biol.* **152**, 92–103.
- Matsko, N.B. (2007) Atomic force microscopy applied to study macromolecular content of embedded biological material. *Ultramicroscopy*, **107**(2–3), 95–105.
- Midgley, P.A. & Weyland, M. (2003) 3D electron microscopy in the physical sciences: the development of Z-contrast and EFTEM tomography. *Ultramicroscopy*, **96**, 413–431.
- Miller, M.K. (2000) *Atom-probe Tomography: Analysis at the Atomic level*. Kluwer Academic/Plenum Press, New York.
- Mou, J., Yang, J. & Shao, Z. (1995) Atomic force microscopy of cholera toxin B-oligomers bound to bilayers of biologically relevant lipids. *J. Mol. Biol.* **248**, 507–512.
- Obst, M., Dittrich, M. & Kuehn, H. (2006) Calcium absorption and changes of the surface microtopography of cyanobacteria studied by AFM, CFM and TEM with respect to biogenic calcite nucleation. *Geochem. Geophys. Geosyst.* **7**, 1–15.
- Reimer, L. (1993) *Image Formation in Low-Voltage Scanning Electron Microscopy* (ed. by D. O'Shea). SPIE Optical Engineering Press, Washington D.C. **TT12**.

- Reviakine, I., Bergsma-Schutter, W. & Brisson, A. (1998) Growth of protein 2-D crystals on supported planar lipid bilayers imaged in situ by AFM. *J. Struct. Biol.* **121**, 356–361.
- Reynolds, E. (1963) The use of lead citrate at high pH as an electron-opaque stain in electron microscopy. *J. Cell Biol.* **17**, 208–212.
- Roessler, F., Grossenbacher, R., Stanicic, M. & Walt, H. (1991) Correlative histological and ultrastructural study of unusual changes in human tracheobronchial epithelium. *Laryngoscope*. **101**, 473–479.
- Sawyer, L.C. & Grubb, D.T. (1996) *Polymer Microscopy*. 2nd ed. Alden Press, Oxford.
- Scheuring, S., Ringler, P., Borgina, M., Stahlberg, H., Müller, D.J., Agre, P. & Engel, A. (1999) High resolution AFM topographs of the *Escherichia coli* water channel aquaporin. *EMBO J.* **18**, 4981–4987.
- Schmitt, L., Ludwig, M., Gaub, H.E. & Tampe, R. (2000) A metal-chelating microscopy tip as a new toolbox for single-molecule experiments by atomic force microscopy. *Biophys. J.* **78**, 3275–3285.
- Schwarz, H. (1994) Immunolabelling of ultrathin resin sections for fluorescence and electron microscopy. *Electron Microscopy 1994 ICEM 13-Paris Les editions de physique, Les Ulis, France* (ed. by B. Jouffrey & C. Colliex), **3**, 233–256.
- Sutton, S.R., Newville, M. & Rivers, M.L. (2003) Synchrotron X-ray microscope analysis. *Geophys. Res. Abstracts*. **5**, 13260.
- Van Harreveld, A. & Crowell, J. (1964) Electron microscopy after rapid freezing on a metal surface and substitution fixation. *Anat. Rec.* **149**, 381–386.
- Walters, D.A., Cleveland, J.P., Thomson, N.H., Hansma, P.K., Wendman, M.A., Gurley, G. & Elings, V. (1996) Short cantilevers for atomic force microscopy. *Rev. Sci. Instrum.* **67**, 3583–3590.
- Walz, T., Tittmann, P., Fuchs, K.H., Müller, D.J., Smith, B.L., Agre, P., Gross, H. & Engel, A. (1996) Surface topographies at subnanometer-resolution reveal asymmetry and sidedness of aquaporin-1. *J. Mol. Biol.* **264**, 907–918.